

# HASP 2016

## UNF-UND Payload OSPA (Ozone Sensors Payload and its Applications)

### Monthly Status Report for September 2016

#### UNF Team

##### **Faculty Advisor:**

Dr. Nirmal Patel

Email: [npatel@unf.edu](mailto:npatel@unf.edu)

Phone: 904-620-1670, Cell: 904-200-2855

#### UND Team

##### **Faculty Advisor:**

Dr. Ron Fevig

Email: [rfevig@aero.und.edu](mailto:rfevig@aero.und.edu),

Phone: 701-777-2480, Cell: 520-820-3440

#### **UNF-UND Students Team:**

	<b>Name</b>	<b>Gender</b>	<b>Ethnicity</b>	<b>Race</b>	<b>Status</b>	<b>Disability</b>
<b>University of North Florida Students Team</b>						
1	Ken Emanuel Cell: 904-614-2117 <a href="mailto:kennecom@gmail.com">kennecom@gmail.com</a>	Male	Non-Hispanic	Caucasian/White	UG-Electrical	No
2	Jesse Lard Cell: 850-348-3510 <a href="mailto:jesselard@gmail.com">jesselard@gmail.com</a>	Male	Non-Hispanic	Caucasian/White	UG-Physics	No
3	Chris Farkas Cell:904-413-6047 <a href="mailto:N00965140@ospreys.unf.edu">N00965140@ospreys.unf.edu</a>	Male	Non-Hispanic	Caucasian/White	UG-Electrical	No

- (1) The HASP2016 balloon flight was successfully launched on Thursday, September 1, 2016 from the NASA-CSBF, Fort Summner, NM. HASP2016 balloon flight had about 20 hours flight time.
- (2) All ozonen sensors, heaters, temperature sensors and pressure sensor worked well during the flight and measured the data.

- (3) Our UBLOX GPS worked well first time during the flight. There was no block of data communications during the flight. The antenna of GPS was mounted on the gondola instead of the top of payload body.
- (4) We have received our payload back after the recovery of HASP2016. We have tested the payload and found that the payload is not damaged and working in the good conditions.

**Some of the plots of data analysis and results are given in this report.**

Fig. 1 shows the HASP 2016 balloon flight profile. The altitude profile was measured by our payload GPS. Our UBLOX GPS worked very well during the flight. We did not need to switch to HASP GPS. The average altitude was around 37015 m during the float.

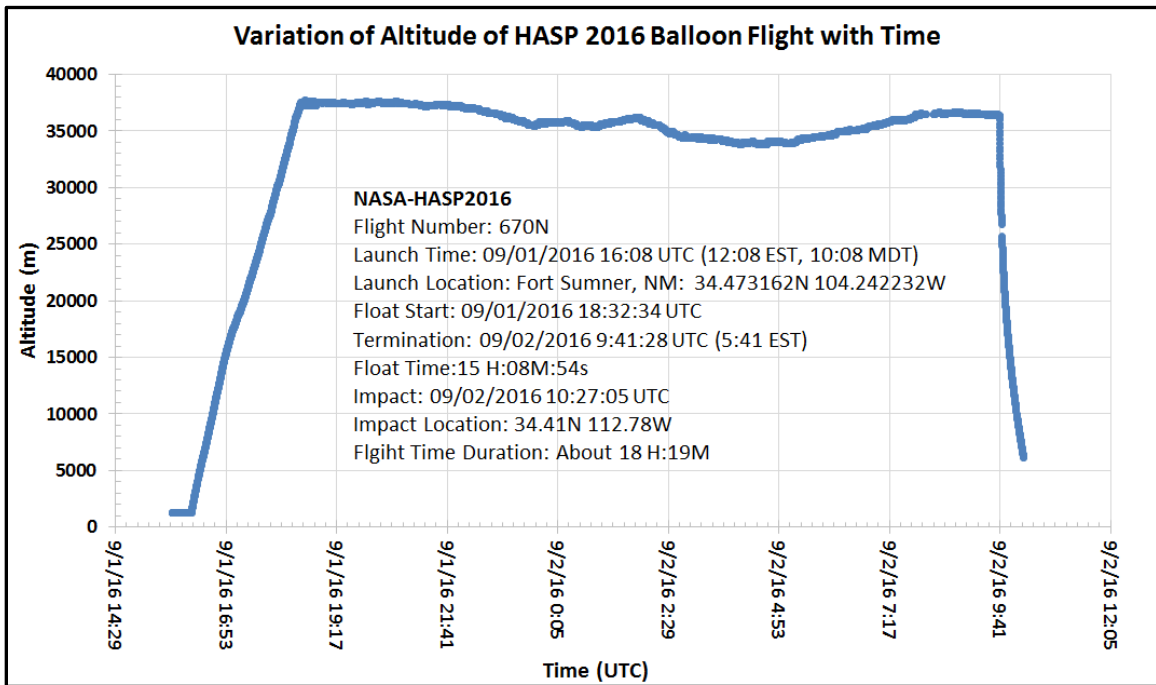


Fig.1 HASP2016 flight profile

Fig.2 (a) shows the variation of pressure with the altitude during the flight. Pressure was measured by a pressure sensor mounted on the PCB of the payload. It was found that the pressure was decreased with increase of the altitude up about 17 km and then nearly saturate with increase of altitude up to the float. The saturation of pressure around 100 mbar was due to the technical limitation of our pressure sensor. We were not able to change it this year but will replace this pressure sensor with one having lower mbar range in the next balloon flight.

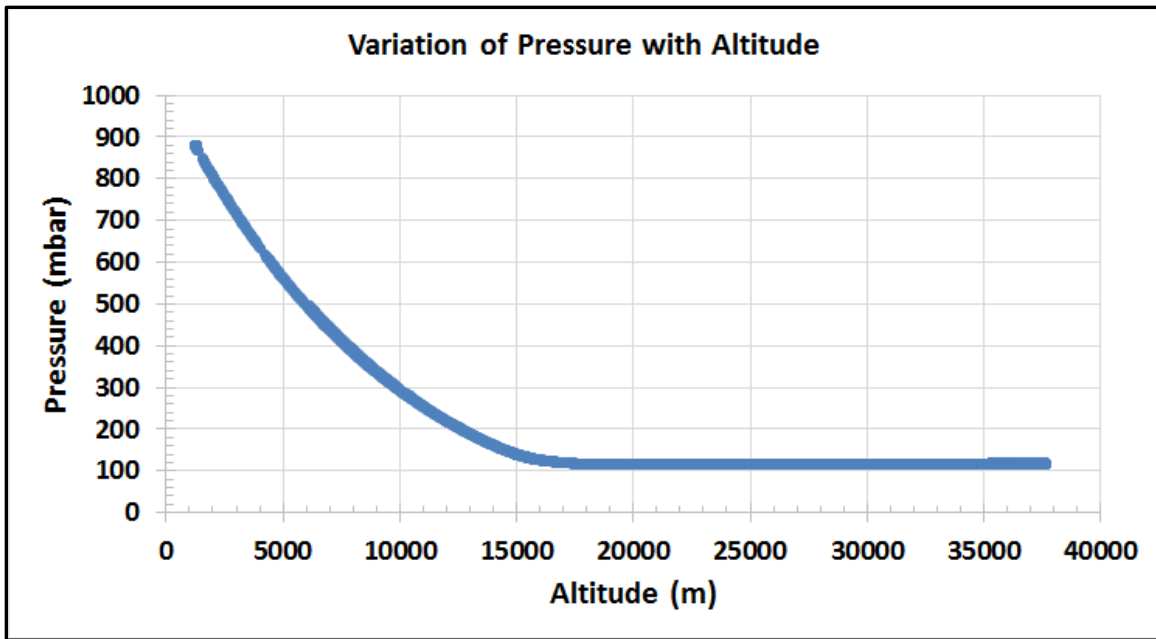


Fig.2 (a) Variation of pressure with altitude

Fig. 2(b) shows the variation of pressure measured by the payload with the flight time (UTC). It shows change of pressure with time during ascending and termination of the flight.

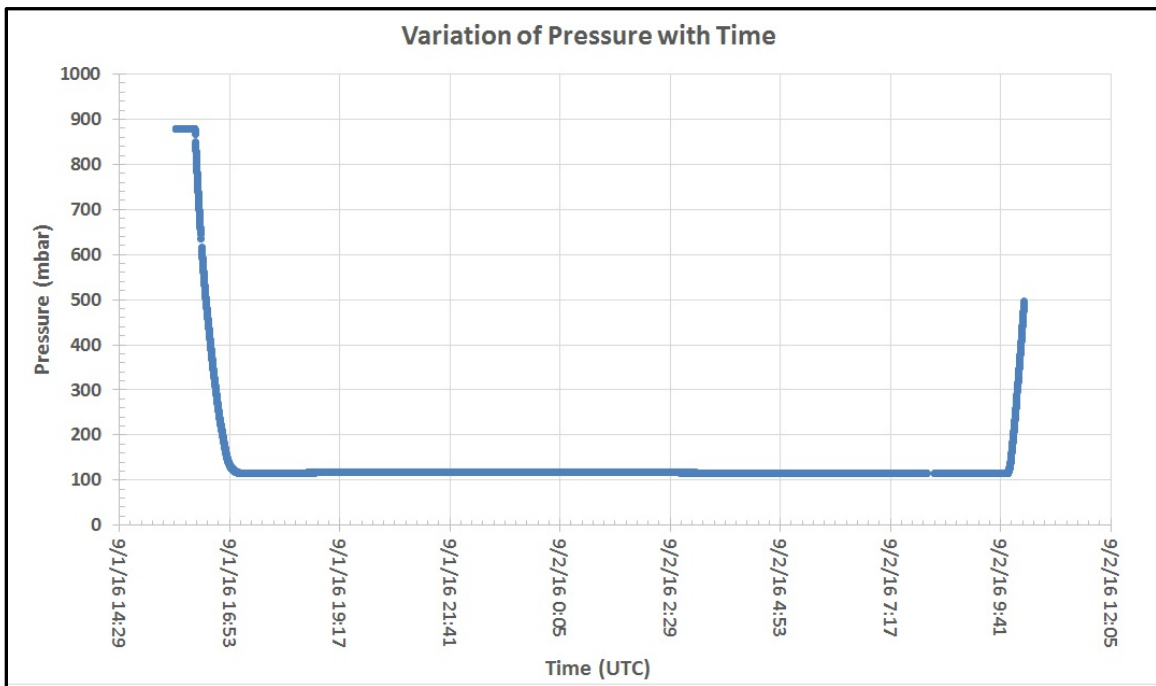


Fig.2 (b) Variation of pressure with time

### 9.3 Power budget during the flight

Fig.3 shows the voltage applied to the payload during the flight. It was found that applied average voltage remain nearly constant about 3320 mV.

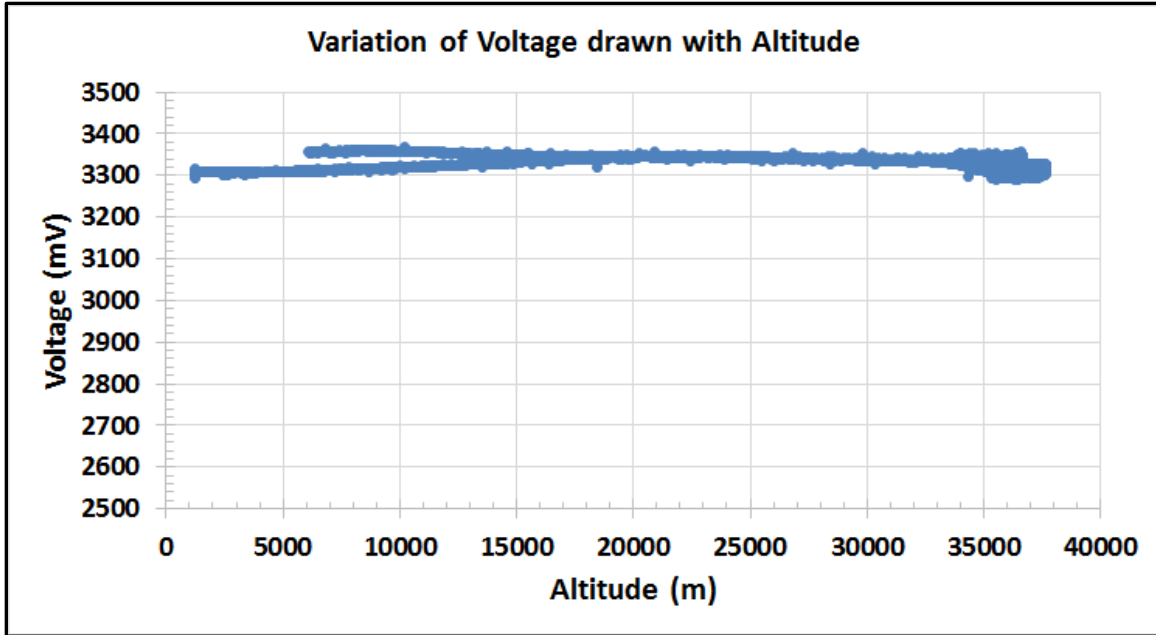


Fig.3 Voltage applied to the payload during the flight.

The current drawn by the payload during the flight is shown in fig. 4.

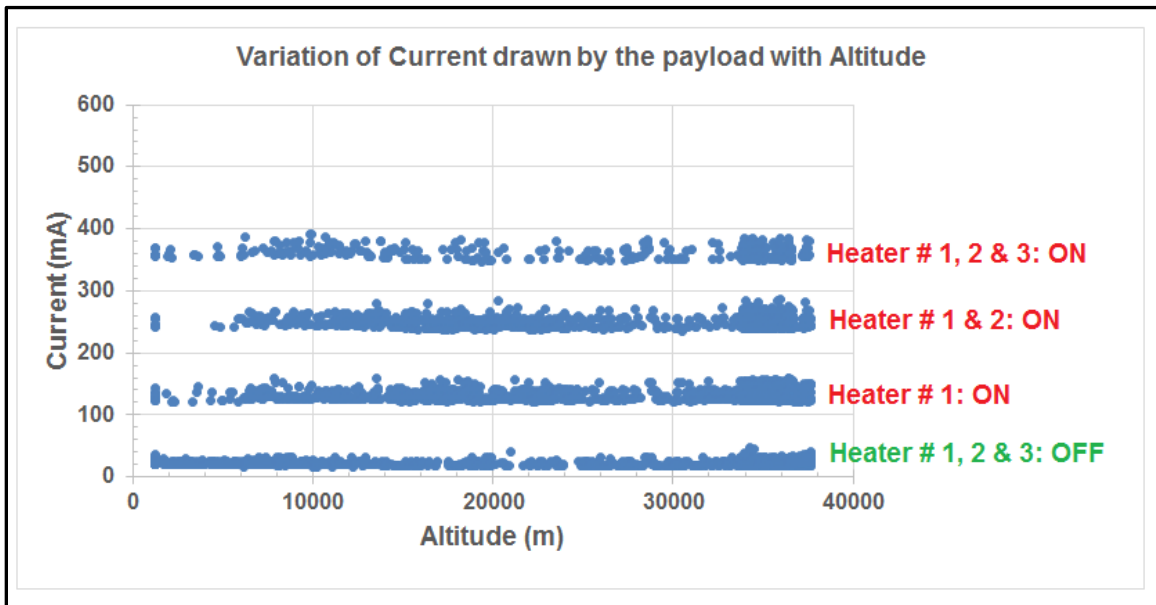


Fig.4 Current drawn by the payload during the flight

The current drawn by the payload during the flight was

- (i) About  $30 \pm 5$  mA when all three heaters were off,
- (ii) About  $140 \pm 10$  mA when Heater #1 ON,
- (iii) About  $250 \pm 10$  mA when Heater # 1 and 2 ON and
- (iv) About  $360 \pm 20$  mA when all three heaters were ON.

The power budget was maintained under the upper limit of HASP requirement during the flight.

#### 9.4 Thermal stability of the payload

The variation of temperature of ozone sensors box #1, 2 and 3 with altitude during the flight is shown in fig.5 (a) to (c), respectively. The temperature of sensors was controlled in the range of  $302 \pm 5.7$  K using an On-Off controller, a polyimide flexible heater (MINCO make) and a temperature sensor (TMP 36). Temperature of sensors was well controlled during the most of time of the flight.

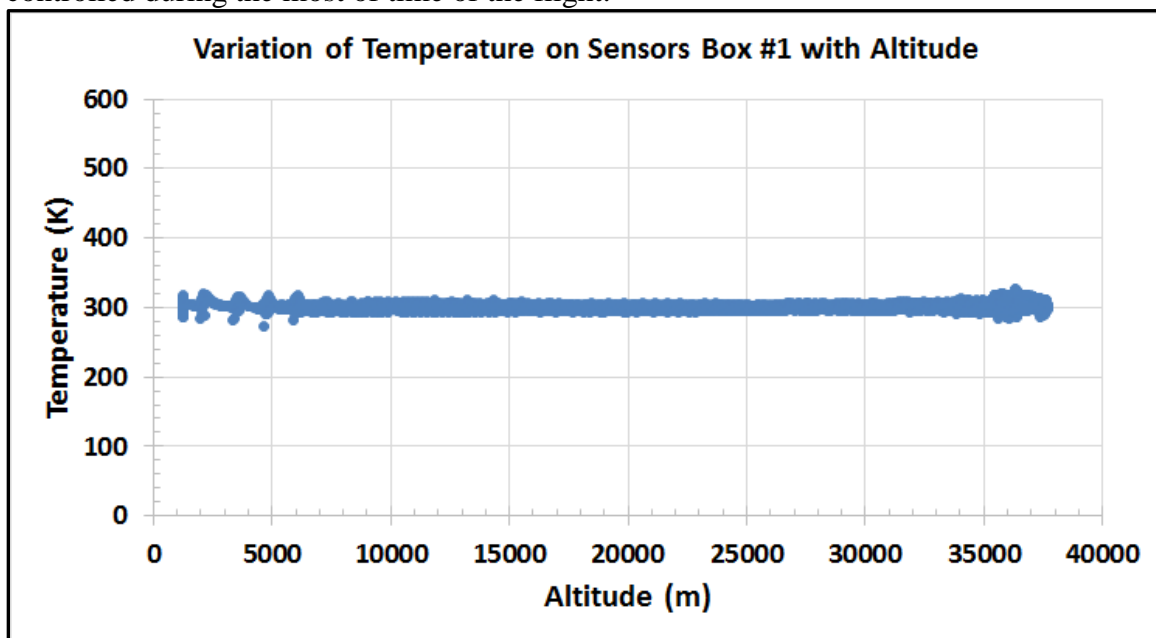


Fig.5 (a) Variability of temperature of ozone sensors in box#1 with altitude

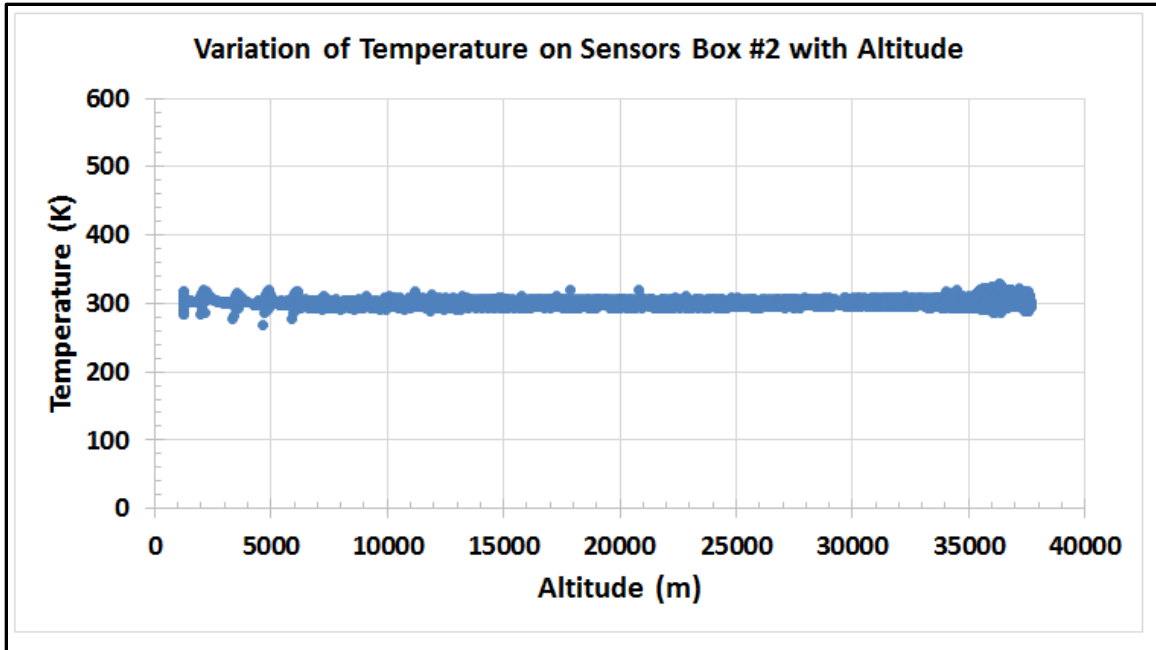


Fig.5 (b) Variation of temperature of ozone sensors in box#2 with altitude

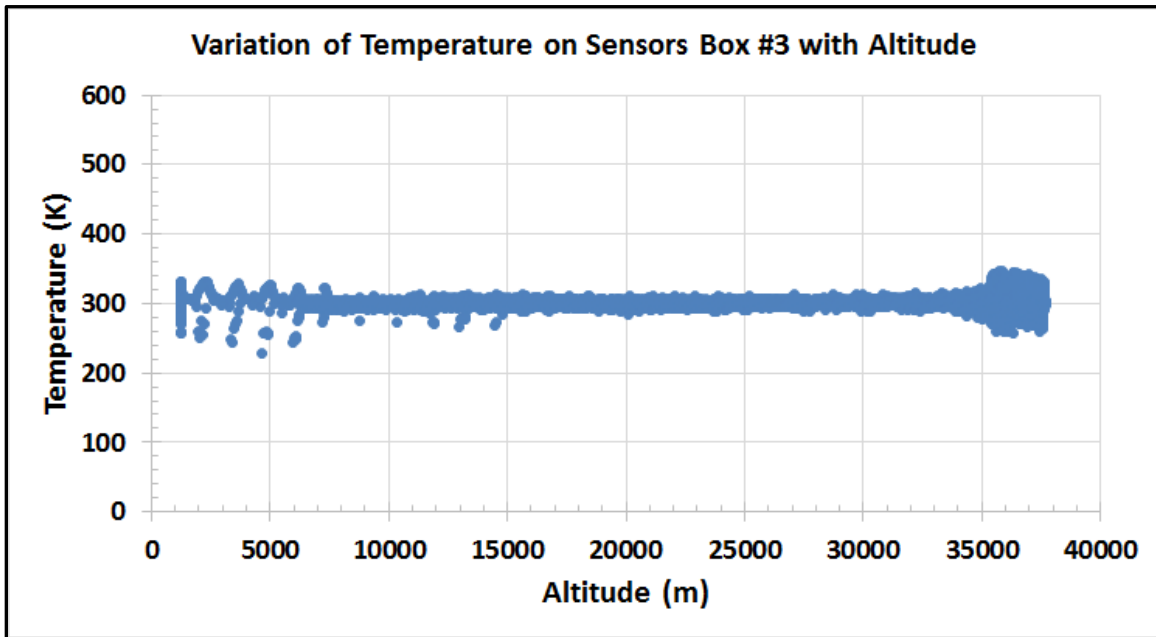


Fig.5 (c) Variation of temperature of ozone sensors in box#3 with altitude

Table-1 shows the measured average temperature, standard deviation and one sigma standard error of temperature of sensor box#1, 2 and 3.

Sensors Box #	1	2	3
Average Temperature (K)	303.9	304.2	305.9
Standard Deviation (K)	6.3	6.7	10.4
Standard Error (K)	0.05	0.06	0.09

Table 1. Average temperature and standard deviation of temperature of sensors array 1, 2 and 3 during the flight.

Variation of temperature of ozone sensors in box#1, 2 and 3 with time (UTC) is shown in the fig. 6(a), (b) and (c), respectively. All three plots shows the reasonable stability of temperature of ozone sensors in the box # 1, 2 and 3. It was observed that temperature of sensors in box #3 got more variation during float, particular at night time.

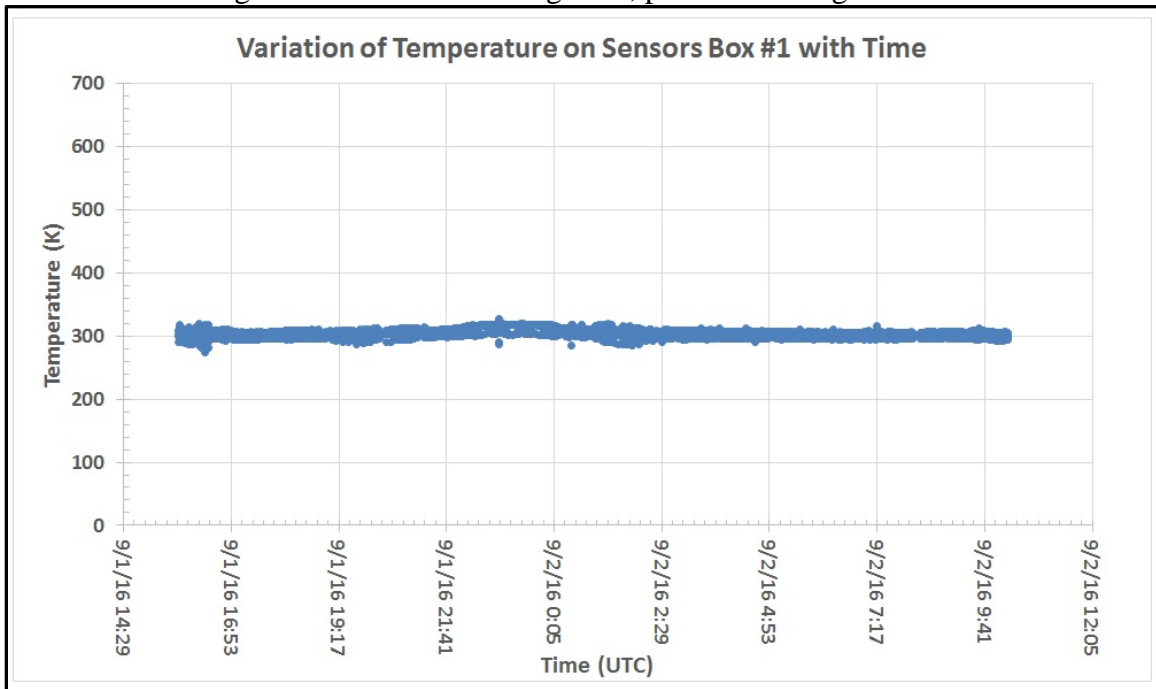


Fig.6 (a) Variation of temperature of ozone sensors in box#1 with time (UTC)

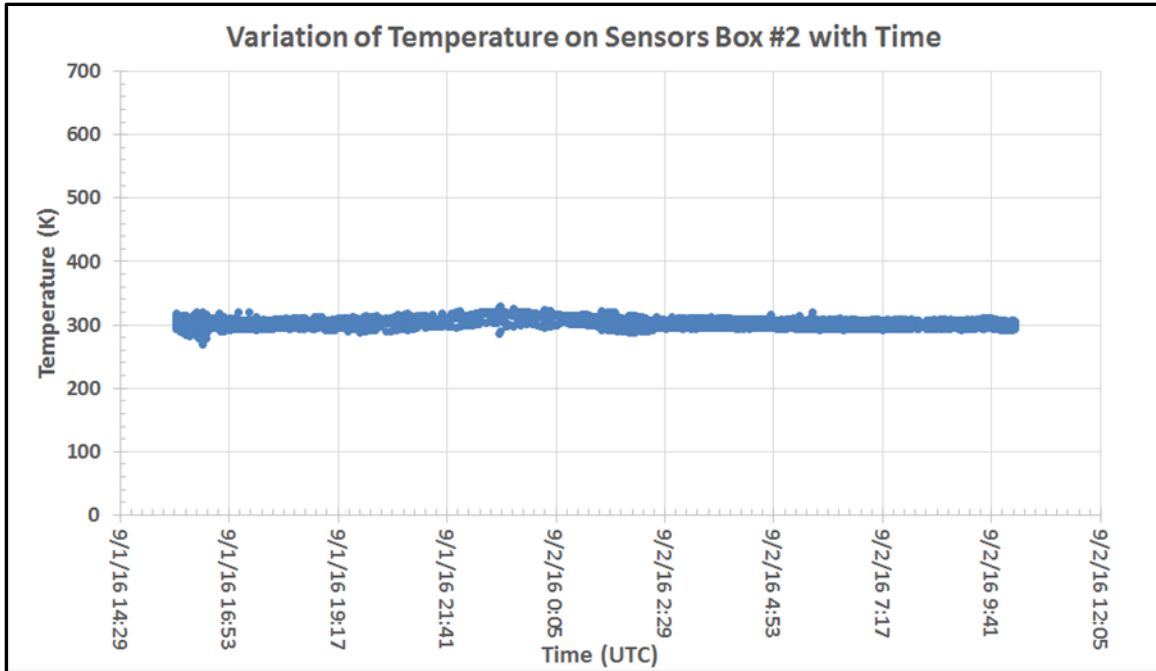


Fig.6 (b) Variation of temperature of ozone sensors in box#2 with time (UTC)

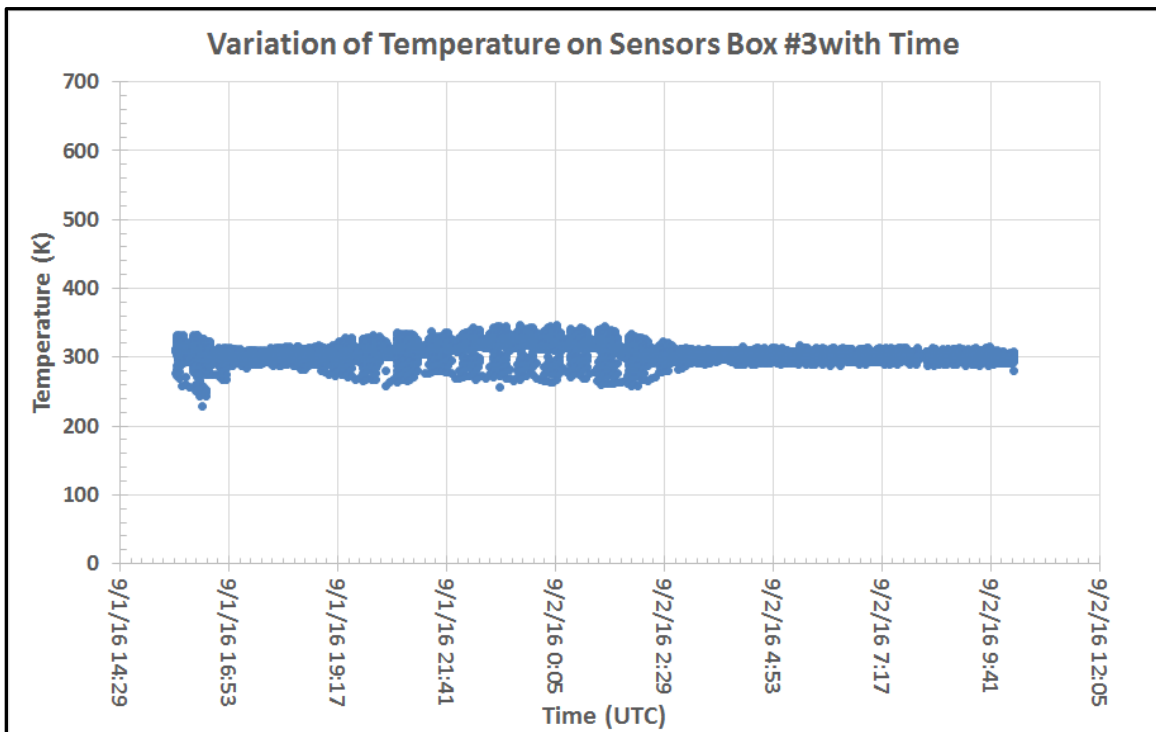


Fig.6 (c) Variation of temperature of ozone sensors in box#3 with time (UTC)

The variation of temperature on central processing unit (CPU) of a microprocessor chip was also measured with altitude and is shown in fig.7. The average temperature  $\pm$  standard



deviation was about  $295 \pm 24$  K. The variation in temperature was observed during due to change of day to night as well as change in altitude too. In addition, the temperature of CPU was reasonably stable within standard deviation. Thus, the thermal stability of our payload is proved and good.

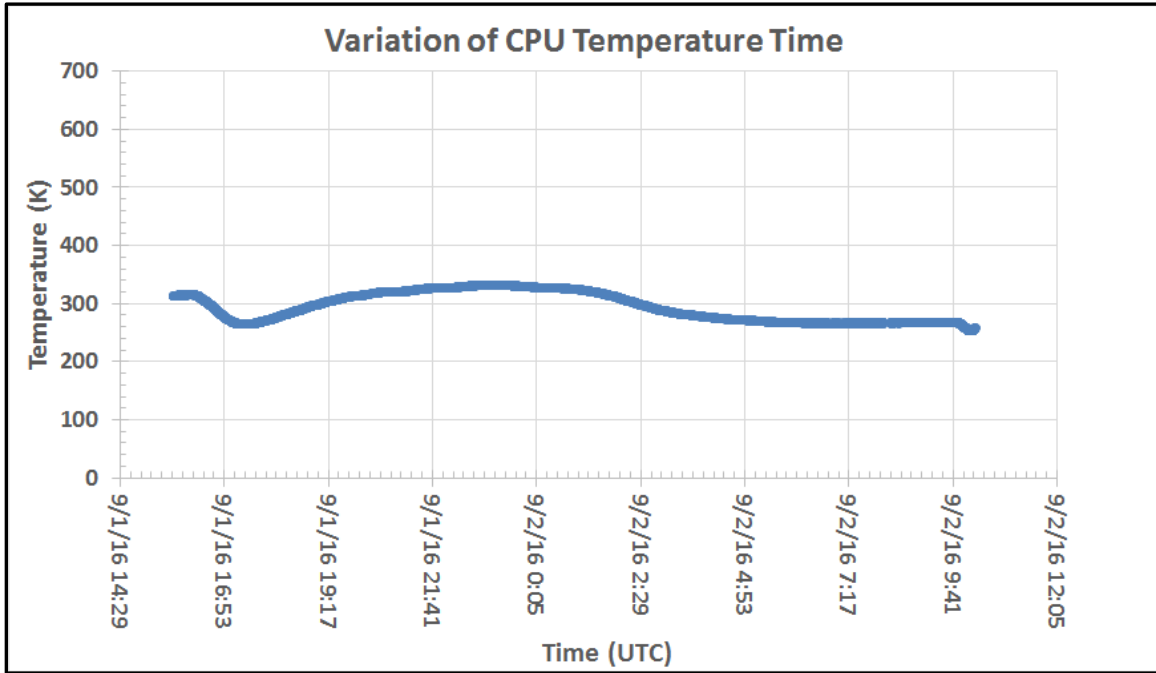


Fig.7 shows variation of temperature on CPU with altitude.

Fig. 29 Variation of ambient temperature on outside skin of UNF payload (Courtesy: Mr. Doug Granger, LSU-HASP)

### Measurements of photovoltage profile during the flight

The variation of photovoltage generated by the photo diodes mounted on sensor box #1, 2 and 3 during the flight is shown in fig 8 (a), (b) and (c), respectively. It was observed that measured photovoltage was larger in the altitude range from 15,000 to 25,000 m. The larger photovoltage confirmed the presence of ultra violet Sun light. In the presence of that UV light oxygen converted into ozone gas. It was also observed a secondary small peak after termination of the flight. The larger photovoltage confirmed the presence of ultra violet Sun light. In the presence of that UV light oxygen converted into ozone gas.

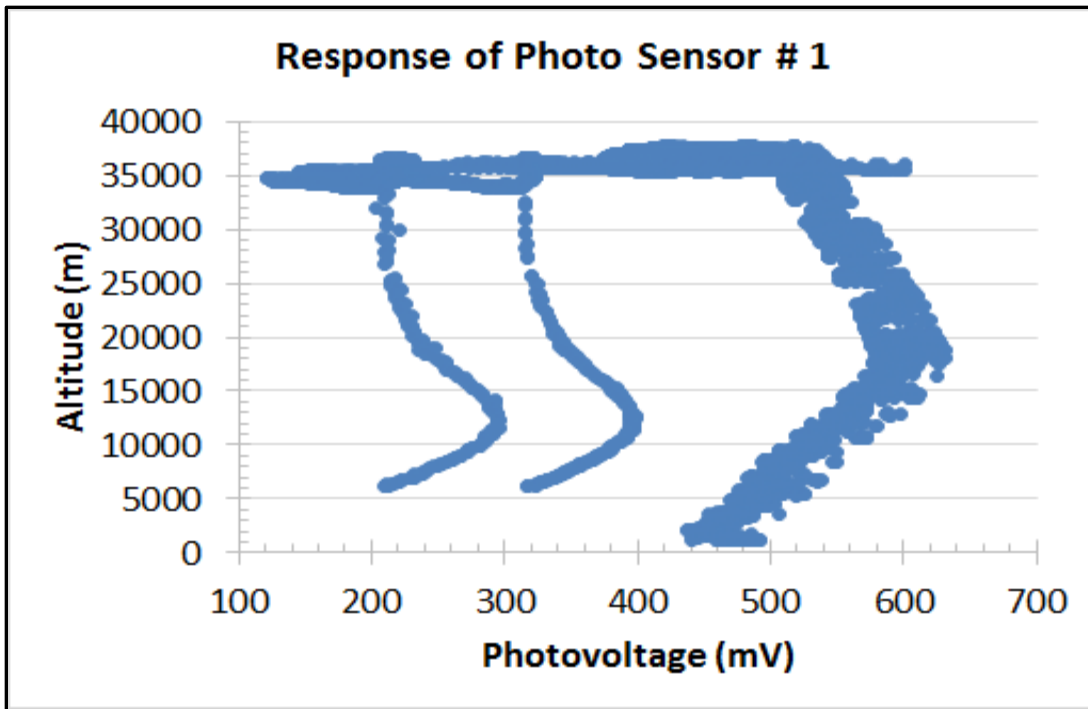


Fig.8 (a) Variation of photovoltage on sensor box#1

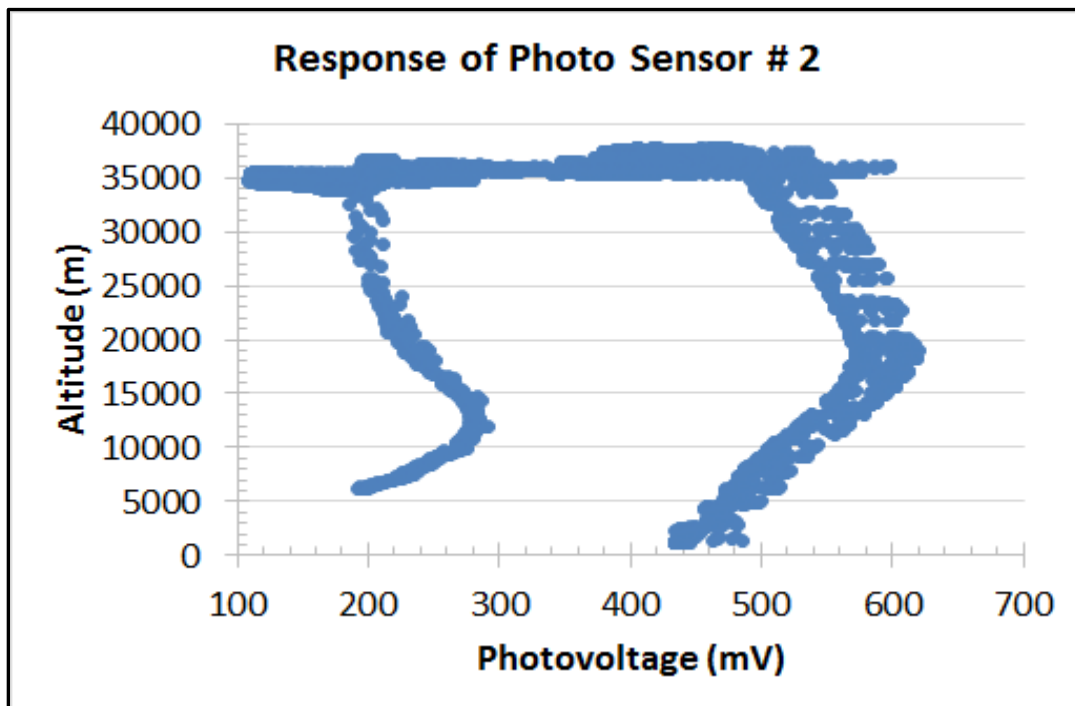


Fig.8 (b) Variation of photovoltage on sensor box#2

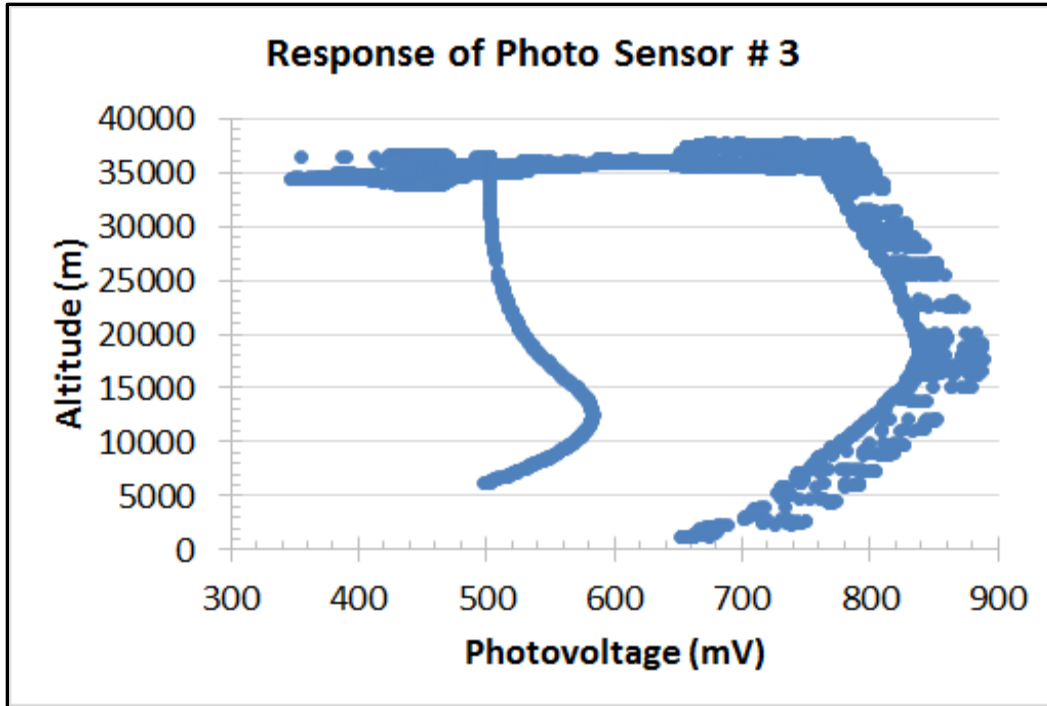


Fig.8 (c) Variation of photovoltage on sensor box#3

The variation of photovoltage generated by the photo diodes mounted on sensor box #1, 2 and 3 with the flight time (UTC) is shown in fig 9 (a), (b) and (c), respectively. Four major zones are shown in Fig. 9 as (i) ascending during day, (ii) float during day, (iii) float during night and (iv) termination. The photovoltage was maximum and shown a peak in the middle of stratosphere. The photovoltage has several spikes during float in day time due to the balloon flight was traveling towards east direction. The photovoltage was decreased and stable during float in the night time. The small peak of photovoltage was observed during after termination of flight and descend journey of flight towards the Earth surface. All three photo sensors have nearly similar response. Photo sensor #3 has large magnitude of photovoltage due to higher sensitivity compare to that of other two photo sensors # 1 and 2.

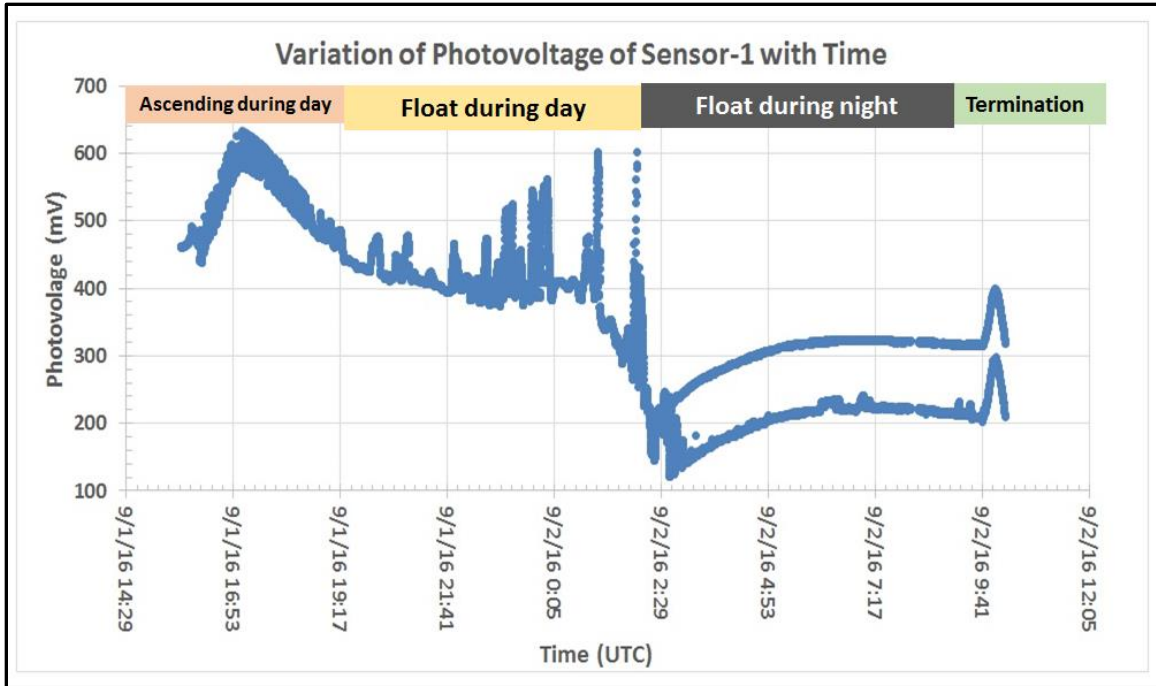


Fig.9 (a) Variation of photovoltage on sensor box#1 with time

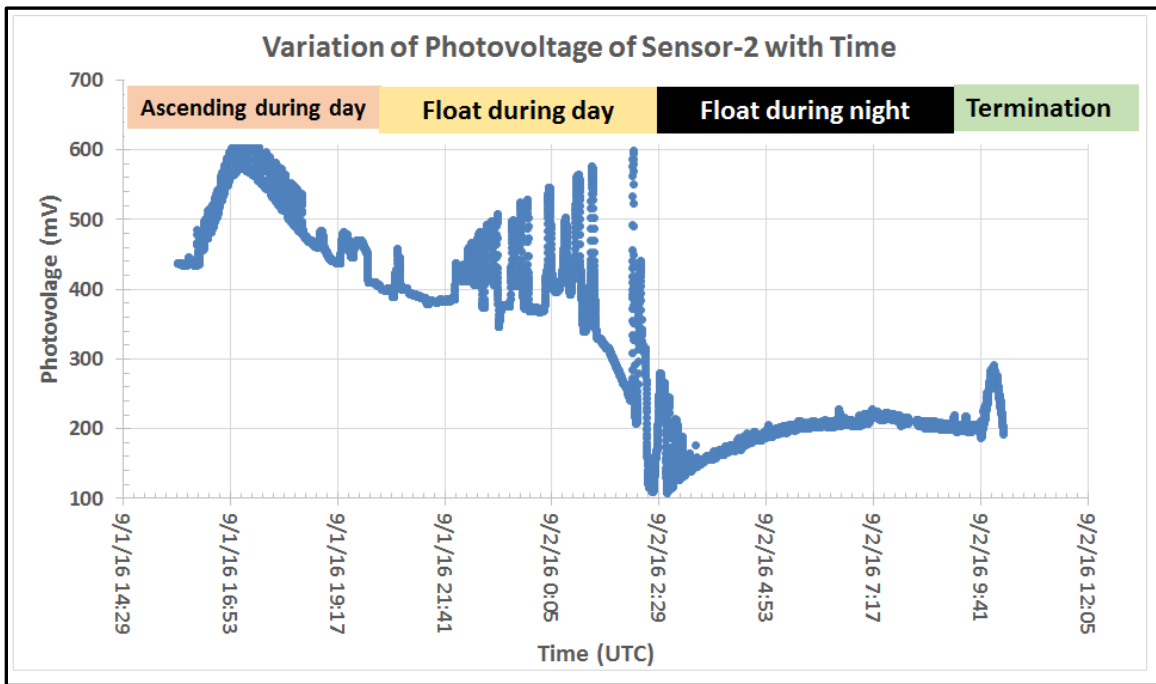


Fig.9 (b) Variation of photovoltage on sensor box#2 with time

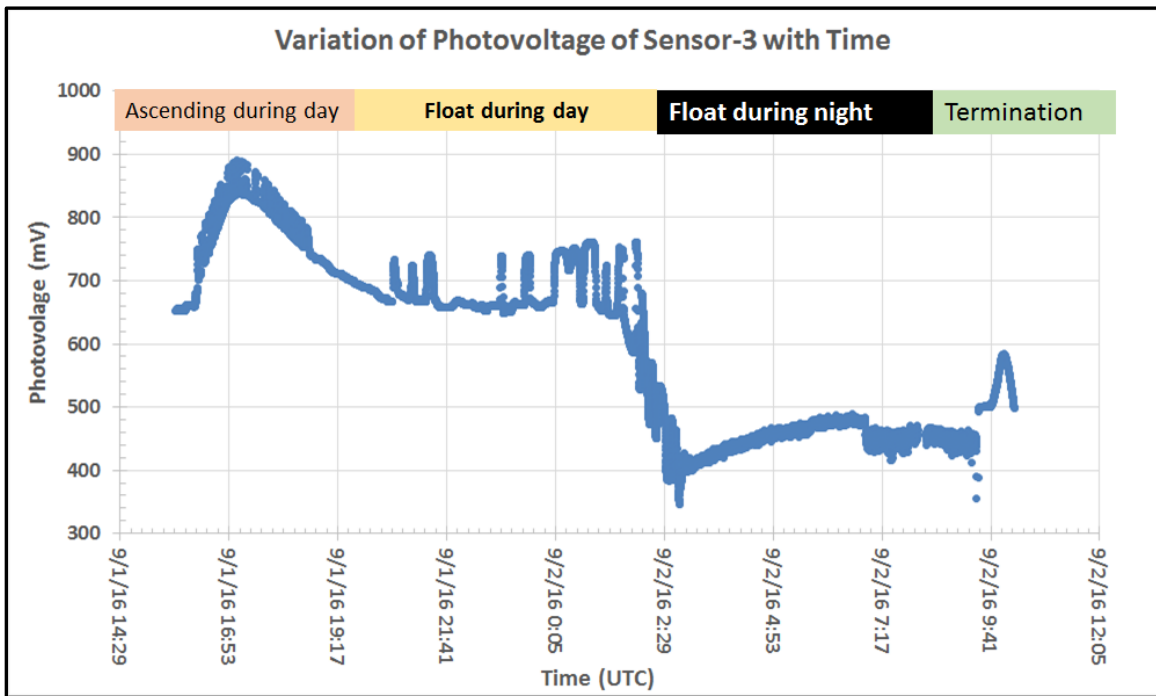


Fig.9 (c) Variation of photovoltage on sensor box#3 with time

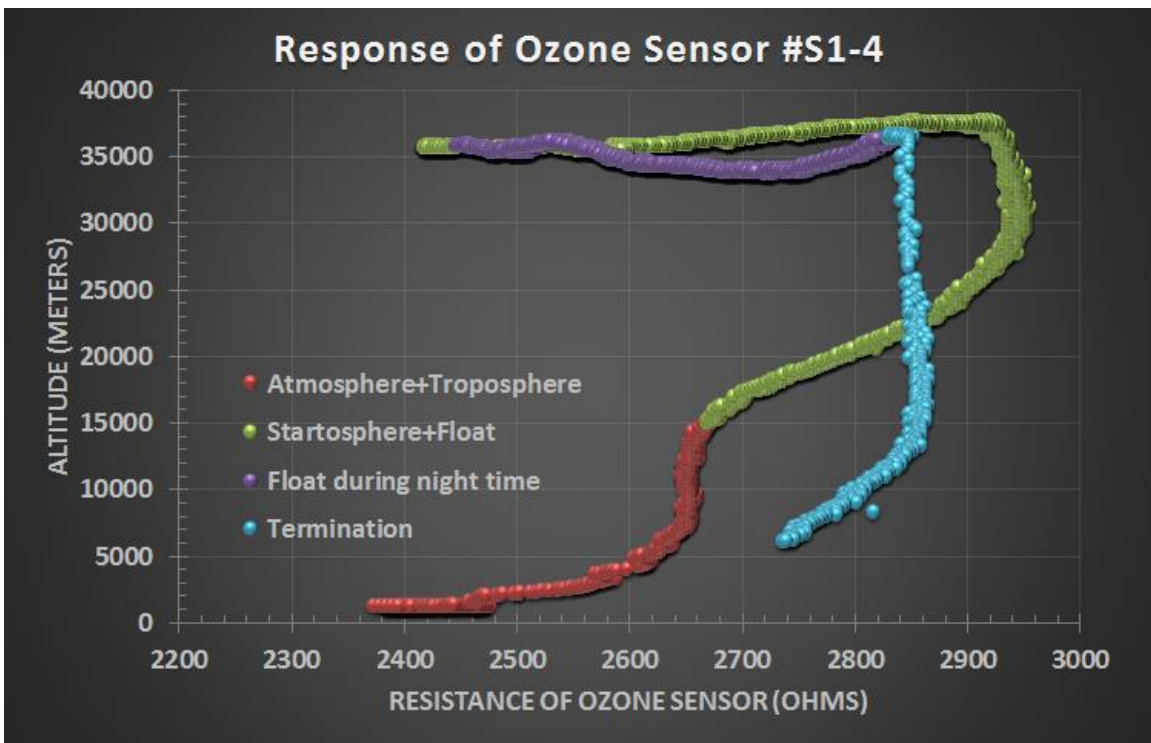


Fig.10 Response of ozone sensor of **Box#1** (#S1-1) with complete range of altitude

Sensor # S1-4 was randomly picked for the discussion of response of sensor with the entire range of altitude of balloon. Sensors of Box-1 were made of improved version of nanocrystalline ITO thin films compare to our previous balloon flights. These sensors have better selectivity and sensitivity with ozone gas.

Small peak of ozone (red color part in fig. 10) was observed during ascending of balloon flight at the altitude below 13000 m. This range of altitude is in the troposphere. This small ozone peak is known as the bad ozone, which is mainly due to the generation of smog in the early morning due to pollution by the automobile vehicles and industries. The bigger peak of ozone is observed at altitude above 25000 m to 37000 (green color part in fig.10). This is due to the ozone in the stratosphere. This ozone is known as good ozone. In the presence of ultra violet light from Sun, oxygen converted into ozone gas. The concentration of ozone is higher in the middle of stratosphere in the presence of ultra violet light. Ozone is oxidizing gas and its concentration depends on amount of available Sun light. Upon adsorption of charge accepting molecules at the vacancy sites from ozone oxidizing gas, the electrons are effectively depleted from the conduction band of n-type Indium tin oxide (ITO) semiconductor sensor. Thus, this leads to an increase in the electrical resistance of n-type ITO gas sensor. At the maximum float of balloon, the concentration of ozone should be constant, but it may vary due to mixing ratio and availability of ultra violet rays from the sunlight during day time. The concentration of ozone decreased slowly (purple color part in fig.10) during float in the night time. After termination of balloon, the payload again entered into the middle of stratosphere, the resistance of sensor should again increase and then decrease. Therefore, a small peak was observed after termination of the balloon flight (blue color part in the fig.10).

Fig. 11 shows the variation of resistance of ozone sensor #S1-4 with time (UTC).

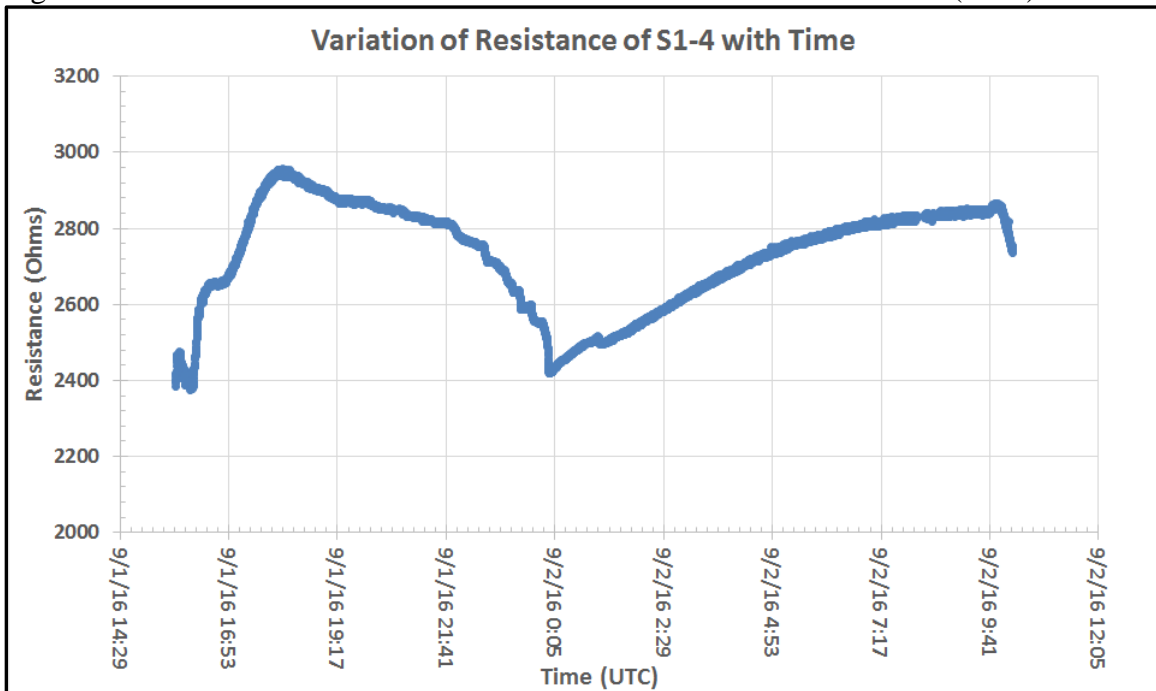


Fig.11 Variation of resistance of ozone sensor of **Box#1** (#S1-4) with time (UTC)

Remaining plots and results will be given in the next month report.